

ARCHITECTURE AND ALGORITHMS FOR REAL-TIME ISAR IMAGING OF DYNAMIC TARGETS

J. Trischman

Naval Command, Control and Ocean Surveillance Center RDT&E Div
53560 Hull Street, San Diego, CA 92152

ABSTRACT

The Naval Command, Control and Ocean Surveillance Center RDT&E Division (NRaD) has been using a 500 MHz Linear Frequency Modulated (LFM) radar to collect measurements of flying aircraft. These data have been used to generate high resolution Inverse Synthetic Aperture Radar (ISAR) images of the targets [1]. Digital Signal Processing (DSP) hardware has been added to the radar and algorithms have been implemented to perform ISAR processing on the data in real time. A VME bus architecture has been developed to provide a scaleable, flexible platform to test and develop real-time processing software. Algorithms have been developed from a system model, and processing software has been implemented to perform pulse compression, motion compensation, polar reformatting, image formation, and target motion estimation.

Keywords: Radar, Imaging; ISAR; Aircraft, Linear Frequency Modulation.

1. INTRODUCTION

NRaD has a long history of generating inverse synthetic aperture radar images of ships and aircraft using wide-band, coherent radars [2][3]. ISAR processing of radar data has many advantages. ISAR images may be used for target identification or to determine target configuration. The processing also provides coherent integration gain that will enhance target detection. ISAR processing has test range applications performing diagnostic measurements of targets and determining specification compliance.

Advances in digital signal processing (DSP) technology make it possible to perform ISAR processing in a computer processor that is embedded in the radar system and generates ISAR images at the rate that the radar signals are being received. This means that a radar operator is able to view target images as the target is being illuminated by the radar.

The NRaD Radar Branch is developing a test bed system to aid in the development of the architecture and algorithms needed to perform real-time ISAR processing. This system is described, and initial results are presented.

2. DESCRIPTION OF LFM RADAR

The NRaD LFM radar is a wide band, coherent, high range resolution radar that operates at X-band. It generates a linear frequency modulated waveform with 500 MHz bandwidth and a 600 ns pulse width. Time-domain sampling of the received signal and digital pulse compression yield a range resolution of 0.5 meters over a range window of up to 1200 m. Table 1 summarizes the radar parameters.

LFM Radar Parameter Summary	
Bandwidth:	500 MHz
Pulse Width:	600 ns.
Center Frequency, f_C :	9.25 GHz
Transmit Power, P_T :	1000 W (peak)
Pulse Frequency, PRF:	50 - 2000 Hz
Receiver Noise Figure, F_N :	6 dB
Sample Frequency, f_S :	500 MHz
Digitizer Dynamic Range:	12 bits (72 dB)
Spurious Free Dynamic Range:	30 dB
Range Resolution:	0.5 m. (3 ns.)

Table 1.

The radar is located on the west side of Point Loma, overlooking the Pacific Ocean, at approximately 120 feet above sea level. This allows the dynamic measurement of aircraft at ranges of 1 to 5 miles and altitudes of 200 to 2800 feet. Ship targets can also be measured at ranges of 3 to 8 nmi. Reference 2 contains a summary of the characteristics of the measurement site.

2.1 RADAR DATA COLLECTION

The LFM Radar uses a surface acoustic wave (SAW) filter to generate a "chirp" signal that sweeps from

1050 MHz to 1550 MHz in 600 ns. This is mixed to an X-band center frequency of 9.25 GHz and transmitted. The received signal is mixed back to a center frequency of 1300 MHz. The signal is then quadrature phase detected by mixing it with the 1300 MHz IF reference signal. This yields an in-phase (I) and a quadrature-phase (Q) signal, each of which has a 250 MHz bandwidth. This process of *baseband conversion* allows for the minimum sampling frequency while still achieving the Nyquist rate [4].

The in-phase and quadrature-phase detected signals are sampled and digitized at the Nyquist rate of 500 MHz per channel. The sample clock is coherent with the master oscillator, and the PRF and range trigger are integral numbers of sample periods, so the time and phase delay from the transmitted pulse to each sample are known. When triggered, the digitizer can capture 4096 I-Q sample pairs. This corresponds to an 8 ms time window (1200 m. range window). This window size is selectable; however, it must exceed the transmitted pulse length plus the delay extent of the target. The digitized waveform is transferred into the memory of a microprocessor-controlled data collection system.

3. ISAR THEORY

An ISAR image is an estimate of the radar reflectivity of a target with respect to a spatial coordinate or coordinates. A one-dimensional image where the coordinate lies along the line-of-sight from the radar to the target is called a *range profile*. Typically in the case of two-dimensional images of aircraft, two orthogonal coordinates are assumed to lie in a (nearly) horizontal plane that contains the target and the radar. The origin is located at an arbitrary point on the aircraft.

A target is typically modeled as a collection of small, "point scatterers." Each scatterer reflects the transmitted signal scaled in amplitude and delayed by $2R_i/c$, where R_i is the range to the i^{th} scatterer. The received signal is the sum of the reflections of each scatterer:

$$s(t) = \sum_{i=1}^N \sqrt{\sigma_i} / R_i^2 \cdot p(t - 2R_i/c), \text{ or}$$

$$S(\omega) = \sum_{i=1}^N \sqrt{\sigma_i} / R_i^2 \cdot P(\omega) e^{-j2\omega R_i/c}$$

where $p(t)$ is the transmitted signal, $P(\omega)$ is its Fourier Transform, and σ is the "radar cross-section" of the scatterer [3][4].

3.1 ONE-DIMENSIONAL IMAGE MODEL

A *target function* can be defined to represent $\sqrt{\sigma}$ as a function of some spatial coordinate system. Let $h(R-R_0)$ be the target function where R_0 is the range to an arbitrary fixed point on the target. Then,

$$S(\omega) = \int_{-\infty}^{\infty} \frac{1}{(R_0+r)^2} h(r) P(\omega) e^{-j\omega 2(R_0+r)/c} dr$$

If R_0 is much larger than the target extent, then

$$S(\omega) = \frac{1}{R_0^2} e^{-j2\omega R_0/c} P(\omega) \int_{-\infty}^{\infty} h(r) e^{-j\omega 2r/c} dr$$

$$= \frac{1}{R_0^2} e^{-j2\omega R_0/c} P(\omega) H(2\omega/c)$$

Thus, when the term which represents the effects of target range is removed, the remaining target response is the convolution of the transmitted signal with the target function: $s(t) = p(t) * h(t \cdot c/2)$. The one-dimensional imaging process involves inverting this relation to estimate $h(r)$ from $s(t)$. This is a deconvolution operation [4].

3.2 TWO-DIMENSIONAL IMAGE MODEL

The geometry for the two-dimensional case is shown in figure 1. The target function, $h(x,y)$, has a two-dimensional spatial Fourier Transform of $H(k_x, k_y)$. If the target is illuminated by a plane wave, the R in the above equations can be replaced with $R_0 - x \cos \theta - y \sin \theta$.

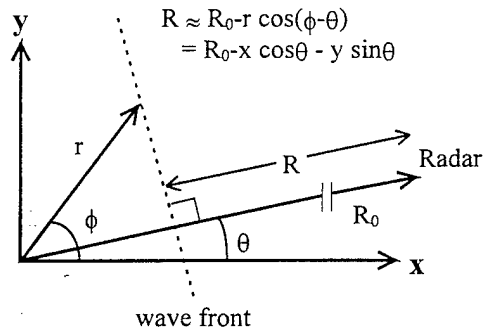


Figure 1. Two-Dimensional Image Geometry

Integrating over the target yields a result similar to one-dimensional case.

$$S_{\theta}(\omega) = \frac{1}{R_0^2} e^{-j2\omega R_0/c} P(\omega) H\left(\frac{-2\omega}{c} \cos \theta, \frac{-2\omega}{c} \sin \theta\right)$$

Solving for ω and θ yields

$$\omega = \frac{1}{2} c \sqrt{k_x^2 + k_y^2}, \quad \theta = \tan^{-1}(k_y / k_x).$$

This shows that ω and θ are polar coordinates in the target function's spatial frequency domain. Again, the imaging problem involves inverting the above equation to obtain an estimate of $h(x,y)$.

4. ALGORITHMS

For each received pulse, a vector of N digitized I and Q samples is collected. The sampled representation of the complex received signal, $s(t)$, is $s_n = I_n - jQ_n$. When a Discrete Fourier Transform (DFT) is applied, the result is a sampled representation of $S(\omega)$. Because of the baseband conversion process, these samples, S_n , correspond to the radar frequencies from $f_c - f_s/2$ to $f_c + f_s/2$, in steps of f_s/N .

Pulsed radars illuminate the target (and collect received data) periodically over time. However, this time scale is a much larger than the one used to characterize the transmitted and receive signals. It is convenient to define a *slow-time* variable, u . Functions of u , such as target range and incidence angle (θ) can be considered constant with respect to *fast-time*, t . A frame of data consisting of M pulses, each having N samples will form an M×N matrix where each row contains the successive samples of a pulse, separated in time by 2 ns., and the rows contain successive pulses, separated by the pulse repetition interval (PRI) of 5 to 100 milliseconds.

4.1 PULSE COMPRESSION

The inversion (imaging) process for either model above involves evaluating the equation,

$$H(\omega) = R_0^2 e^{j2\omega R/c} P(\omega)^{-1} S(\omega).$$

This is most easily implemented in the frequency domain. $P(\omega)^{-1}$ is realizable only if the transmitted signal is infinite in bandwidth. It is approximated by a function, $G(\omega)$, that is non-zero over the band where $P(\omega)$ is non-zero. When $G(\omega) = P(\omega)^*$ it is a matched filter. $G(\omega)$ can also be a pulse compression filter. When applied to the transmitted pulse, this filter should result in an "ideal" compressed pulse with a linear phase spectrum and an amplitude spectrum equal to a frequency weighting function chosen to meet sidelobe requirements [5].

The pulse compression filter is derived from samples of the transmitted pulses that are routed through the receiver and collected in the same manner as $s(t)$. Pulse compression is performed by Fast Fourier Transform (FFT) of each received pulse, multiplication by the

compression filter function, and then inverse FFT. The resulting range profile is the target function convolved with $p(t)*g(t)$. Thus the shape of this function determines the range resolution of the image. For a bandpass signal with bandwidth β , the resolution is approximately $c/2\beta$. A trade-off between resolution and maximum sidelobe level can be set by the choice of amplitude weighting function.

4.2 MOTION COMPENSATION

The next step in image generation is motion compensation, the process of removing the effects of the target's radial motion. For each pulse, the range to the origin point on the target contributes the term $1/(R^2 e^{j2\omega R/c})$ to the spectrum of the received signal. In principle this can easily be removed if the range is known for each pulse. The phase, however, is sensitive to relative range errors of less than $\lambda/4$, (< 1 cm at X-band), so range must be accurately estimated. The range, $R(u)$, is modeled as a third order polynomial (i.e., range, velocity, acceleration, and jerk) over an image frame. The compensation is performed while the data is in the frequency domain.

4.3 RANGE-DOPPLER IMAGE

After motion compensation, any amplitude or phase modulation due to radial motion of the target will have been removed. However, if the target is rotating, the relative range of scatterers that are offset in cross-range from the origin will change over successive pulses. The change in range will be $2k_{u1}\sin(\Delta\theta)$, where k_{u1} is the cross-range distance to the scatterer. If the angle change is small, and the rotation rate, θ' , is constant, then the response of that scatterer will have a constant frequency Doppler modulation.

$$h(u) = h(0)e^{-j2\omega k_{u1}u\theta'/c}$$

Range-Doppler images are generated at this stage by taking the Fourier Transform with respect to u . (i.e. an FFT by column).

$$H(k_u) = h(0)\delta(k_u + 2\omega k_{u1}\theta'/c)$$

This results in the response of the scatterer being shifted in the k_u or *cross-range* direction. The resulting image shows target reflectivity as a function of range in one dimension, and Doppler frequency in the other dimension. Scatterers rotating towards the radar have positive doppler frequency, and those rotating away have negative frequencies.

The range-doppler image has several uses. When the assumptions made above are valid, $H(r, \lambda k_r/2\theta)$ is a good approximation of $h(x,y)$, where x is aligned with the radar line-of-sight. In addition, θ' does not have to be known to generate the image. If the rotation rate (θ) is not known, however, then cross-range dimensions cannot be calculated. This reveals an ambiguity that is inherent in the two-dimensional imaging geometry.

Since processing over u (slow-time) involves successive radar pulses, the pulse frequency (PRF) of the radar is the sampling frequency, and thus it determines the maximum Doppler frequency that can be resolved without aliasing. A range-doppler image allows this aliasing to be directly observed. In addition, errors in estimating the target's velocity cause an offset of the entire image in the k_u dimension. This effect can be used as an aid in refining motion estimates.

4.4 TWO DIMENSIONAL IMAGING

Several factors contribute to errors in the range-doppler image. As the change in angle increases, non-linear components of scatterer motion causes phase error. In addition, if the change in range of a scatterer exceeds the range resolution, the scatterer's response is smeared. The image becomes blurred as the distance from the origin increases. Compensating for these effects is accomplished by inverting the two-dimensional image model.

Pulse compression and motion compensation of a frame of data results in a matrix, $H_{m,n}$, consisting of samples of $H(u, \omega)$. If the target's rotation, $\theta(u)$, is known or can be estimated, then an angle can be assigned to each response, resulting in $H(\theta, \omega)$. The data then represents the target's reflectivity as a function of frequency and rotation angle. Data in this form are said to be polar-formatted, because frequency and rotation angle form polar coordinates in the spatial frequency domain, $H(k_x, k_y)$. To generate a focused ISAR image, the data must be polar-reformatted. The FFT algorithm requires evenly spaced data samples, and polar-formatted data are normally not. Therefore, the data must be resampled at points on an evenly spaced rectangular grid in the k_x, k_y space. A two-dimensional inverse FFT is then applied to recover $h(x,y)$ [2].

In the resampling technique currently used for LFM data, each row of frequencies is interpolated to find evenly spaced points in down-range spatial frequency. Then each column of the new data is interpolated to

find evenly spaced points in cross-range spatial frequency [3].

5. SYSTEM ARCHITECTURE

The NRaD Real-Time ISAR System is based around a VME bus [6]. This allows various modular system components such as processors, memory, and interface boards to be added. The system configuration is shown in figure 2.

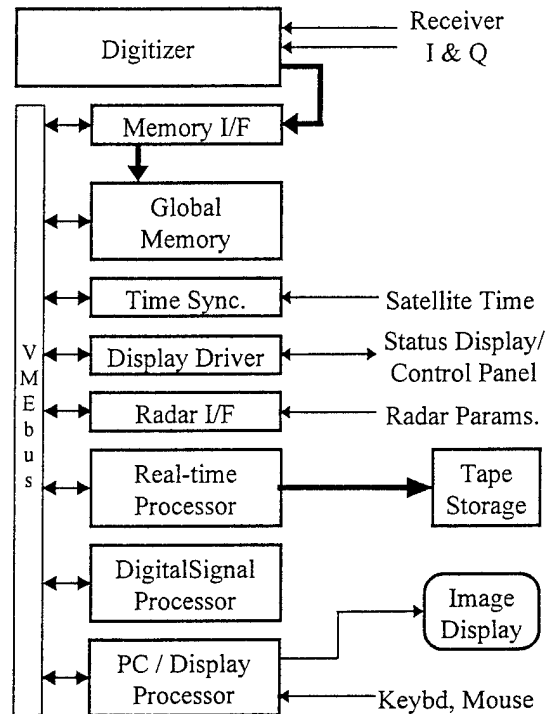


Figure 2. NRaD Real-Time ISAR System

Digitized samples of the received pulse are transferred by the Memory Interface card to the Global Memory card via a dedicated VSB bus. This can be done in parallel with transfers over the VME bus. The time synchronization board generates time tags for each pulse. The CRT card is used to drive a touch-screen status and control panel. The Radar Interface card is used to read parameters from the radar and provide control outputs. The Real-Time Control Processor coordinates system activity through the above I/O cards, manages data buffers, and outputs the data to 8-mm tape for later analysis.

The Digital Signal Processor (DSP) card performs the ISAR processing algorithms. It operates on data samples stored in global memory, and puts results back into global memory. The card contains two ADSP-

21020 processors operating at a 33-MHz clock frequency. This results in a peak processing rate of 67 million floating point operations per second on each processor.

The Display Processor generates waveform and image displays from the processed data in global memory. It is a PC compatible computer that is also used for software development and debugging. Because the system is based on a bus architecture, its capabilities can be expanded by adding additional DSP or display processor cards in the spare slots.

5.1 DATA FLOW

Figure 3 shows the flow of data through the Real-Time ISAR processing algorithms.

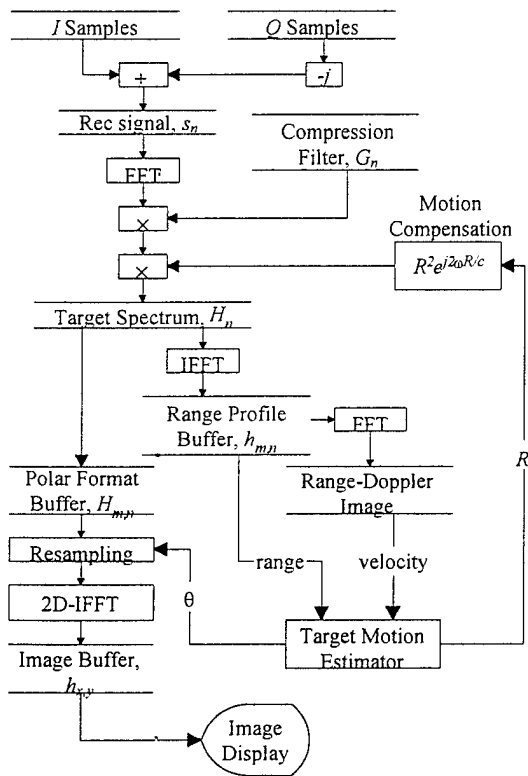


Figure 3. Real-time ISAR Data Flow

I and Q samples of the received signal are read from global memory and combined into a complex vector, s_n . The vector is Fast Fourier Transformed to S_n and multiplied by the pulse compression and motion compensation vectors, resulting in the target spectrum. A range profile, h_m , is generated by IFFT and saved in a buffer for display and range tracking purposes. A prominent scatterer is tracked and used as the origin

point for the image. The range delay of this point is fed into the motion estimation filter.

A sequence of range profiles can also be processed to form a range-doppler image. This is the least computationally intense image, and is useful for target acquisition and tracking. When range-doppler images are generated, the doppler frequency of the prominent scatterer is determined and used to calculate a velocity correction to the target motion estimate.

Next the target spectrums are collected in a frame buffer to form $H_{m,n}$. A rotation estimate is used to calculate the interpolation points. Currently the resampling process does not attempt to rotate the x and y axes to an orientation aligned with line of flight. Therefore the image still shows range on one axis and cross-range on the other. The resampling also assumes a constant rotation rate as well. A 2-D IFFT of the interpolated values results in an estimate of $h(x,y)$. The displayed image is the magnitude of $h_{m,n}$, scaled in dB.

6. RESULTS

Currently the algorithms described above are being tested, and the software to implement them is being transferred from a workstation to the digital signal processors. The data being processed are raw samples that were recorded on 8-mm tape by the LFM radar. These samples were collected from stationary calibration targets, small boats, commercial airliners, and military jets. The use of pre-recorded data allows testing without requiring the radar or targets to be available.

Typically the digitizer collects 1024 I and 1024 Q samples per pulse at 500 MHz. This results in a 2 μ s sample time, which assures that the entire return signal is sampled, even when only coarse tracking is being used. Transferring this data to global memory takes about 1 ms. Transferring it to the DSP memory also requires 1 ms. These transfers are done by dedicated hardware, and occur in parallel with the signal processing.

The first DSP performs the following functions:

- 1) convert integer samples to complex, (190 μ s),
- 2) Fourier Transform, (590 μ s),
- 3) calculate range phase vector, (125 μ s),
- 4) evaluate motion compensation exp., (2,920 μ s),
- 5) multiply compression filter and motion compensation vector, (250 μ s),
- 6) inverse Fourier Transform, (800 μ s),
- 7) square vector, (65 μ s),

- 8) find peak index, (100 μ s),
- 9) and copy data to buffers, (125 μ s).

This requires a total processing time of about 5.2 milliseconds. A design goal is to process pulses at 200 Hz that would allow less than 5 ms of processing per pulse. A significant portion of the time is taken evaluating the exponential in the motion compensation term. At the end of each pulse processing cycle, the target spectrum and range profile data reside in memory buffers which are accessible to the second DSP. After a frame of data is accumulated, it performs the next steps in the algorithm while the first processor fills a second buffer.

A typical frame size for commercial aircraft is 256 pulses, just over 1 second. A 256 point FFT requires 130 μ s. With copying and computing power, a 256 x 256 range-doppler image can be generated in 45 milliseconds. If the target is small this can be reduced further. The image data must be scaled to a byte value and written to the memory of a display card in order to be viewed. This still allows an image update rate of 10 Hz.

The two-dimensional inverse FFT required for the focused image requires about 100 ms. In addition the polar sampling must be performed. Since sampled range is generally 8 or more times longer than the target, the data in the ω domain (rows) is over-sampled. Thus a linear interpolation between adjacent point will yield good results. For each pulse, an angle, θ_m is assigned. The k_x sample for each frequency ω_n is taken at $\omega = \omega_n / \cos \theta_m$.

The k_y samples are found by interpolating along the θ dimension (columns). The samples are taken at a spacing of $\Delta\theta = \Delta k_y \omega_0 / \omega_n$. Since the data is not over-sampled in the θ domain, this interpolation is performed in the workstation environment using an FFT, zero padding, and an IFFT. This approach is too computationally intensive for a real-time environment. In addition, evaluating the polar to rectangular mapping in cases where rotation is not uniform poses an additional challenge.

7. CONCLUSIONS

There are definite advantages to a real-time imaging capability in high resolution, coherent radars. The architecture developed at NRaD shows promise in providing this. Additional work is required in implementing the classical imaging equations in a computationally efficient manner. Two areas that show

room for improvement are the evaluation of the phase exponential used for motion compensation and interpolation for polar resampling.

8. ACKNOWLEDGEMENTS

This work was made possible by funding from the Office of Naval Research and the Air Force Wright Laboratory. Many members of the NRaD Radar Branch assisted in building and operating the radar. Techniques and software that form the basis for these algorithms have been developed over the last decade by personnel at the Naval Command Control and Ocean Surveillance Center / RDT&E Division, Naval Air Warfare Center / Weapons Division, and Naval Surface Warfare Center.

REFERENCES

1. J. Trischman, S. Jones, R. Bloomfield, E. Nelson, R. Dinger, "An X-Band Linear Frequency Modulated Radar for Dynamic Aircraft Measurement," AMTA Proceedings, pp.431-436, Long Beach, CA, Oct. 1994.
2. Radar Branch. "Radar-Cross-Section Data Collection and Processing Capabilities at NOSC," TD 1802, April 1990 (unclassified).
3. D. R. Wehner, *High Resolution Radar* [Artech House, Boston], 1987.
4. M. Soumekh, *Fourier Array Imaging* [Prentice Hall, Englewood Cliffs, NJ], 1994.
5. Skolnik, ed., *The Radar Handbook*, 2nd edition, [McGraw-Hill Publishing Co., San Francisco], 1990.
6. W. D. Peterson, *The VMEbus Handbook*, 2nd edition, [VFEA International Trade Association, Scottsdale], 1991.